J. Appl. Comput. Mech., 8(1) (2022) 219-231
DOI: 10.22055/JACM.2020.33386.2218

ISSN: 2383-4536
jacm.scu.ac.ir

Shahid Chamran University of Ahvaz

Journal of Applied and Computational Mechanics

Research Paper

Thermal Analysis of Radiating Film Flow of Sodium Alginate using MWCNT Nanoparticles

Akinbowale T. Akinshilo[1], Amin Davodi[2], Adeleke Ilegbusi[3], Gbeminiyi Sobamowo[1]

[1] Department of Mechanical Engineering, University of Lagos, Akoka-Yaba, Nigeria
[2] Department of Civil and Mechanical Engineering, Babol University of Technology, Babol, Iran
[3] Department of Mechanical Engineering, Yaba College of Technology, Yaba, Nigeria

Received April 27 2020; Revised June 01 2020; Accepted for publication June 01 2020.
Corresponding author: A.T. Akinshilo (ta.akinshilo@gmail.com)

Abstract. Heat transfer of fluids plays an important role in process flows, as this has significant impacts in process configurations, energy pricing and utilization. Therefore, this paper, the heat and mass transfer of a radiating non-Newtonian Sodium alginate transported through parallel squeezing plates is examined. The radiating-squeezing fluid flows through the parallel plates arranged vertically against each other with multi walled carbon nanotube (MWCNT) particles. Transport mechanics and thermal conditions of the Sodium alginate is studied using systems of coupled nonlinear models. This higher order, governing ordinary differential models are used to analyze the thermal and mass transfer of the nanofluid using the adomian decomposition method. Results obtained from analytical study displayed graphically are used to investigate effect of thermal radiation on film flow of MWCNT nanoparticles on the Sodium alginate. As revealed from result, concentration increase of MWCNT nanoparticles increases thermal profile significantly. This can be physically explained owing to increasing concentration, increases thickness of thermal boundary due to conductivity enhancement of fluid. Improved thermal diffusivity drops thermal gradient which reduces heat transfer. Whereas, radiation effect on fluid transport shows decrease in heat transfer as thermal conductivity becomes lower than temperature gradient of the flow. Obtained analysis when compared against other methods of solution (numerical and approximate analytical) proves satisfactory. Therefore, the results obtained from the work provides a good basis for the application and improvement of the Sodium alginate in medical, pharmaceutical and manufacturing industries among other practical application.

Keywords: Sodium Alginate, MWCNT particles, heat transfer, fluid transport, Adomian Decomposition Method.

1. Introduction

The study of heat and mass transfer of fluid transport through parallel medium is one of the most important research studies in engineering, science and technology. This is due to its application in modern equipment's including hydraulic lifts, pumps, cooling towers and lubricating system utilized industrially. As this equipment's are of paramount importance to process and energy industries, they can be classified therefore as economic drivers. It becomes imperative to study the controlling parameters of this transport in the bid to enhance thermal and mass transfer, hence improving energy utilized which in turn reduces cost. Utilizing nanofluid in the study of hydrothermal analysis, Hosseinzadeh et al. [1] analyzed magnetohydrodynamic flow using analytical methods. Non-Newtonian natural convective flow through flat plate was presented by Ziabaksh and Domairry [2] using the homotopy analysis method. Mustafa et al. [3] investigated the mass and heat transfer of squeezing flow unsteadily between parallel plates while Jayesimi et al. [4] studied the mass flow of micropolar fluid flowing through a porous channel driven by high mass transfer. Analysis of hydro dynamic non-Newtonian third grade fluid was presented by Adesanya and Falade [5] with porous medium. Hoshyar et al. [6] studied the incompressible Newtonian unsteady flow behavior using analytical method. Liquid- solid interaction of nanofluid was investigated by Ijaz et al. [7] flowing through wavy channel. Analytical study of non-Newtonian fluid was conducted using parallel plates by Kargar and Akbazade [8]. Turkyilmazoglu [9] investigated single- and two-phase lamina film flow through vertically curved walls. Numerical and analytical methods was utilized by Hatami and Ganji [10] in the solutions of natural convective Sodium alginate transport. Comparative analysis of Newtonian and non-Newtonian fluid flow was conducted by Hatami et al. [11] adopting the differential transform method. Stretching plates comprehensive analysis was studied by Ahmadi et al. [12] for heat and mass flow. Squeezing unsteady Eyring -Powell flow in stretching channel was analyzed by Ghadikolaei [13] considering thermal radiation and effect of joule heating. Brownian and thermophoresis parameter effect of unsteady nanofluid flowing through parallel plates was studied by Sheikholeslami et al. [14]. Investigations

Published online: March 28 2021

on nanofluid flow heat transfer under magnetic field and squeezing was conducted by [15-22] in the bid to enhance mass flow in transport mediums. Heat transfer for energy applications considering varying shaped ducts, thermal conditions processes was investigated using experimental techniques [23-29]. Further, [30-35] performed reviews of nanofluid transport using numerical techniques through flow channels.

The importance of nanoparticles in fluid flow and heat transfer cannot be over emphasized as it has been proven that nanoparticles added to base fluid improve the thermal conductivity of the fluid about thrice [36-39]. Moreso, the carbon nanotube (CNTs) nanoparticles are nanoparticles with strong intermolecular bonding, which consist of cylindrically shaped tubes of nanometer size. Since the CNTs are allotropes of carbon they have very strong mechanical property. Its shape, thickness and length depend on the graphene sheet shape. Therefore, a multi walled carbon nanotube nanoparticles are layers of concentric graphene forming a tubular shape. In addition to the mechanical and thermal properties of the CNT. Its finds practical applications in the development of structural and thermal materials, biomedicine and electronic applications amongst others [41-46].

Most practical and yet realistic problems are higher ordered, coupled system of partial or ordinary model equations. In the bid to analyze, examine and study the flow mechanics and thermal properties of the fluid transport numerical and analytical methods have been applied over the years by researchers [46-78]. These methods include the Homotopy analysis method [HAM], homotopy perturbation method [HPM], differential transformation method [DTM], regular perturbation method [RPM], Akbari-Ganji method [AGM] and the weighted residual methods (collocation, Garlerkins and least square method). With these methods having their own linearity, round off errors, discretization, and initial or guess term, strong dependence on perturbation parameter and weak nonlinearity. The adomian method of decomposition [ADM] is selected as the preferred analytical scheme to provide accurate, reliable solution, coupled with fast convergence rate of approximate analytical solution of the nonlinear system of mechanics governing the mass and heat transfer under consideration. Therefore, the ADM been a simplistic approach of analyzing nonlinear model problems by decomposing into linear and nonlinear parts makes the ADM attractive to researchers. As thermal properties of material of construction/ fabrication of nanoparticles plays a pertinent role in heat transfer. The performance of nano crystal was studied by Xiao et al. [79]. Shortly after Lewis et al. [80] investigated the effect of single crystalline nanoparticle using winter bottom constructions. The lattice nematicity of triangular crystalline Iron nanostructure was performed by Little et al. [81]. Single walled carbon nanotube of nonlinear liquid plasmons was studied by Wang et al. [82]. These material were studied and improved in the bid to enhance the performance of nanoparticles during the heat transfer process.

Literatures past, revealed there have been no study on thermal radiating non-Newtonian Sodium alginate flow through parallel plate considering combined squeeze and multi walled carbon nanoparticles (MWCNT) .This paper therefore aims to study the heat transfer effect of combined squeeze and MWCNT particles on radiating thermal flow of the Sodium alginate through a vertical micro-channel, utilizing the adomian decomposition method (ADM).

2. Model Development and Analytical Solution

The steady fluid transport and heat transfer of the Sodium alginate, a non-Newtonian fluid containing the multiwall carbon nanoparticles (MWCNT) flows under natural convection through vertical parallel plates. The squeezing fluid transport moves under natural convection at constant temperature of the walls having opposing magnitude to each other. The distance between the walls is represented as 2b, this is shown in Fig.1, since fluid is incompressible, nanoparticles and base fluid are in thermodynamic equilibrium. As observed from the conditions at the boundary of the plates, the fluid particles closest to the plate and plate have equal velocity whereas temperature of the walls are constant but opposing in magnitude to each other. This causes a rise in temperature at the left plate and a fall at the right plate.

The constitutive relations are formed based on the flow and heat transfer process described above, considering the reasonable assumptions stated. Based on the aforementioned and following the model of the Sodium alginate presented by [11, 22], the combined effect of constant radiating squeeze flow of the base fluid using the MWCNT nanoparticles are stated as:

$$\mu\frac{d^2\upsilon}{dx^2}+6\beta_3\left(\frac{d\upsilon}{dx}\right)^2\frac{d^2\upsilon}{dx^2}+\rho_f\gamma(T-T_m)g=0 \tag{1}$$

$$\mu\left(\frac{d\upsilon}{dx}\right)^2+2\beta_3\left(\frac{d\upsilon}{dx}\right)^4+k\frac{d^2\theta}{dx^2}=0 \tag{2}$$

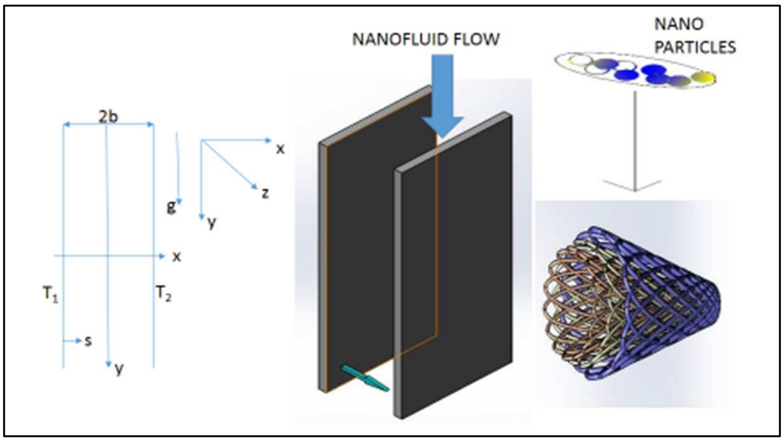

Fig. 1. Physical model of the problem.

where the dimensionless parameters take the forms:

$$\delta = \frac{6\beta_3 \upsilon_0^2}{\mu_f G^2}, A_1 = \frac{\rho_{nf}}{\rho_f}, A_2 = \frac{(\rho C_p)_{nf}}{(\rho C_p)_f}, A_3 = \frac{k_{nf}}{k_f}, Ec = \frac{\rho_f V_o^2}{(\rho C_p)_f (T_1 - T_2)}, Pr = \frac{\mu_f (\rho C_p)_f}{\rho_f k_f}, \theta = \frac{T - T_m}{T_1 - T_2}, S = \frac{\alpha b^2}{2\upsilon}, V = \frac{\upsilon}{V_0}, R = \frac{4\sigma^* T_m^3}{kk^*} \tag{3}$$

where $A_{1\text{-}3}$, are the nanofluid parameters, Ec is the Eckert number, Pr is the Prandtl number, Theta is the dimensionless temperature, S is the squeeze parameter, R is the radiation parameter, S is the squeeze parameter and δ is the dimensionless non-Newtonian parameter. The ranges for the Ec and Pr parameters are selected for laminar and steady flows. The δ parameter at zero connotes Newtonian flow, while δ > 0 denotes non-Newtonian flows. The plates come together when S<0 and recedes or dilates when S>0. Whereas the R parameter is valid for short distance travels according to [39] for R >1.

Effect of radiation on the heat transfer is measured utilizing the Rooseland approximation [39]. The Rooseland approximation is confirmed valid during short travel distance of the radiation before scattering. The approximation stated by Rooseland is given to account for this effect. Since heat transfer due to radiation exit within non-Newtonian fluid before been scattered within thick optical fluid. The heat flux due to radiation is presented as follows:

$$q_r = -\frac{4\sigma^*}{3k}\frac{\partial T^4}{\partial y} \tag{4}$$

Assuming small thermal flow differences, temperature T^4 is expressed linearly. Expanding T^4 using the Taylor series about T_m, which is the free stream temperature. Upon neglecting higher order terms yields $T^4 \cong 4_m^3 T - 3T_m^4$, this can be simply shown as:

$$\frac{\partial q_r}{\partial y} = -\frac{16\sigma^* T_m^3}{3k^*}\frac{\partial T}{\partial y} \tag{5}$$

Utilizing the Non dimensional parameters expressed in Eq. (3). The governing Eqs. (1)- (2) are described as:

$$\frac{d^2V}{dX^2} + 6S\delta A_1\left((1-\phi) + \phi\frac{\rho_{nf}}{\rho_f}\right)(1-\phi)^{2.5}\left(\frac{d^2V}{dX^2}\right)\left(\frac{d^2V}{dX^2}\right)^2 + \theta \tag{6}$$

$$\left(1 + \frac{4}{3}R\right)\frac{d^2\theta}{dX^2} + Ec.PrS\left(\frac{A_2}{A_3}\right)\left(\left((1-\phi) + \phi\frac{\rho_{CNT}}{\rho_f}\right)(1-\phi)^{-2.5}\right)\left(\frac{d^2V}{dX^2}\right)^2 + 2\delta.Ec.Pr.\left(\frac{1}{A_3}\right)\left(\frac{dV}{dX}\right)^4 = 0 \tag{7}$$

The nanofluid parameters are described adopting the heat capacitance $(\rho C_p)_{nf}$, effective dynamic viscosity μ_{nf}, thermal conductivity k_{nf} and effective density ρ_{nf} of the nanofluid are defined as follows [40]:

$$\rho_{nf} = (1-\phi)\rho_f + \phi\rho_{CNT} \tag{8}$$

$$(\rho C_p)_{nf} = (\rho C_p)_f\left[(1-\phi) + \phi\frac{(\rho C_p)_{CNT}}{(\rho C_p)_f}\right] \tag{9}$$

$$A_2 = \frac{\rho C_{nf}}{\rho C_f} \tag{10}$$

$$A_3 = \frac{k_{nf}}{k_f} = \frac{1 - \phi + 2\phi\left(\frac{k_{CNT}}{k_{CNT} - k_f}\right)In\left(\frac{k_{CNT} + k_f}{2k_f}\right)}{1 - \phi + 2\phi\left(\frac{k_f}{k_{CNT} - k_f}\right)In\left(\frac{k_{CNT} + k_f}{2k_f}\right)} \tag{11}$$

Taking the boundary condition as

$$\begin{aligned} \upsilon = 0, \theta = 0.5 \ \text{ at } x = -1 \\ \upsilon = 0, \theta = -0.5 \ \text{ at } x = 1 \end{aligned} \tag{12}$$

The adomian decomposition approximate method of solution will be utilized in generating solution to the system of coupled, higher order, ordinary differential equation. This is an analytical scheme. Utilising the ADM in the applications of the coupled governing nonlinear differentials Eqs. (3-4), may be expressed as:

Table 1. Thermo physical properties of sodium alginate [22] and MWCNTs nanoparticles [40].

	Density (Kg/m³)	Specific heat capacity (J/kgK)	Thermal conductivity (W/mk)
Sodium Alginate (SA)	989	4175	0.637
MWCNT	1600	796	3000

$$L_{xx}(v) = -6\delta SA_1\left((1-\phi)+\phi\frac{\rho_{CNT}}{\rho_f}\right)(1-\phi)^{2.5}\left(\frac{dv}{dx}\right)^2\frac{d^2v}{dx^2}-\theta \tag{13}$$

$$L_{xx}(\theta) = \left(-EcPrS\left(\frac{A_2}{A_3}\right)\left((1-\phi)+\phi\frac{\rho_{CNT}}{\rho_f}\right)(1-\phi)^{-2.5}\left(\frac{dv}{dx}\right)^2-2\delta EcPr\left(\frac{1}{A_3}\right)\left(\frac{dv}{dx}\right)^4\right)/\left(1+\frac{4}{3}R\right) \tag{14}$$

In the bid to simplify the difficult integrations associated with the highest order differential operator, taken as $L_{xx} = d^2/dx^2$ for the coupled equation.Upon inverting L_{xx} gives L_{xx}^{-1}. Thus applying L_{xx}^{-1} to Eqs.(13)-(14) yields

$$v = L_{xx}^{-1}\left[-6\delta SA_1\left((1-\phi)+\phi\frac{\rho_{CNT}}{\rho_f}\right)(1-\phi)^{2.5}\left(\frac{dv}{dx}\right)^2\frac{d^2v}{dx^2}\right]-L_{xx}^{-1}\theta+C_1x+C_2 \tag{15}$$

$$\theta = \left[L_{xx}^{-1}\left[-EcPrS\left(\frac{A_2}{A_3}\right)\left((1-\phi)+\phi\frac{\rho_{CNT}}{\rho_f}\right)(1-\phi)^{-2.5}\left(\frac{dv}{dx}\right)^2\right]-L_{xx}^{-1}\left[2\delta EcPr\left(\frac{1}{A_3}\right)\left(\frac{dv}{dx}\right)^4\right]\right]/\left(1+\frac{4}{3}R\right)+C_1x+C_2 \tag{16}$$

With respect to ADM, velocity and temperature may be expressed in the form

$$v = \sum_{n=0}^{\infty} v_n \tag{17a}$$

$$\theta = \sum_{n=0}^{\infty} \theta_n \tag{17b}$$

The nonlinear terms will be explored in the form of Γ_n and Λ_n in the Adomian polynomials which yields

$$\sum_{n=0}^{\infty}\Gamma = 6\delta SA_1\left((1-\phi)+\phi\frac{\rho_{CNT}}{\rho_f}\right)(1-\phi)^{2.5}\left(\frac{d}{dx}\sum_{n=0}^{\infty}v^2\right)\left(\frac{d^2}{dx^2}\sum_{n=0}^{\infty}v\right) \tag{18}$$

$$\sum_{n=0}^{\infty}\Lambda = \left(EcPrS\left(\frac{A_2}{A_3}\right)\left((1-\phi)+\phi\frac{\rho_{CNT}}{\rho_f}\right)(1-\phi)^{-2.5}\left(\frac{d}{dx}\sum_{n=0}^{\infty}v^2\right)+2\delta EcPr\left(\frac{1}{A_3}\right)\left(\frac{d}{dx}\sum_{n=0}^{\infty}v^4\right)\right)/\left(1+\frac{4}{3}R\right) \tag{19}$$

Utilising Eqs. (18)-(19) the Eqs. (15)-(16) may be expressed as

$$v = -L_{xx}^{-1}\theta - L_{xx}\left(\sum_{n=0}^{\infty}\Gamma\right)+C_1x+C_2 \tag{20}$$

$$\theta = -L_{xx}\left(\sum_{n=0}^{\infty}\Lambda\right)+C_1x+C_2 \tag{21}$$

where the boundary conditions takes the form

$$\begin{aligned}&\sum_{n=0}^{\infty}v_n = 0, \sum_{n=0}^{\infty}\theta_n = 0.5 \quad \text{at } x = -1\\ &\sum_{n=0}^{\infty}v_n = 0, \sum_{n=0}^{\infty}\theta_n = -0.5 \quad \text{at } x = 1\end{aligned} \tag{22}$$

The zeroth order can be obtained from the recursive relations Eqs. (15)- (16)

$$v_0 = C_1x + C_2 - L_{xx}^{-1}\theta_0 \tag{23}$$

$$\theta_0 = C_1x + C_2 + 0 \tag{24}$$

With leading order boundary condition expressed as

$$\begin{aligned}&v_0 = 0, \theta_0 = 0.5 \quad \text{at } x = -1\\ &v_0 = 0, \theta_0 = -0.5 \quad \text{at } x = 1\end{aligned} \tag{25}$$

The remaining order of the solutions is given as

$$v_{j+1} = L_{xx}^{-1}(\Gamma_j), \quad j \geq 0 \tag{26}$$

$$\theta_{j+1} = L_{xx}^{-1}(\Lambda_j), \quad j \geq 0 \tag{27}$$

with boundary condition expressed as

$$\sum_{n=0}^{\infty} \upsilon_n = 0, \sum_{n=0}^{\infty} \theta_n = 0.5 \text{ at } x = -1$$
$$\sum_{n=0}^{\infty} \upsilon_n = 0, \sum_{n=0}^{\infty} \theta_n = 0.5 \text{ at } x = 1 \tag{28}$$

From Eq. (18) the Adomian polynomians, Γ_n can be obtained as

$$\Gamma_0 = 6\delta SA_1\left((1-\phi)+\phi\frac{\rho_{CNT}}{\rho_f}\right)(1-\phi)^{2.5}\left(\left(\frac{d\upsilon_0}{dx}\right)^2\frac{d^2\upsilon_0}{dx^2}\right) \tag{29}$$

$$\Gamma_1 = 6\delta SA_1\left((1-\phi)+\phi\frac{\rho_{CNT}}{\rho_f}\right)(1-\phi)^{2.5}\left(\left(\frac{d\upsilon_0}{dx}\right)^2\frac{d^2\upsilon_1}{dx^2}+2\frac{d\upsilon_0}{dx}\frac{d\upsilon_1}{dx}\frac{d^2\upsilon_0}{dx^2}\right) \tag{30}$$

From Eq. (19) the Adomian polynomians, Λ_n can be obtained as

$$\Lambda_0 = \left(EcPrS\left(\frac{A_2}{A_3}\right)\left((1-\phi)+\phi\frac{\rho_{CNT}}{\rho_f}\right)(1-\phi)^{-2.5}\left(\frac{d\upsilon_0}{dx}\right)^2+2\delta EcPr\left(\frac{1}{A_3}\right)\left(\frac{d\upsilon_0}{dx}\right)^4\right)/\left(1+\frac{4}{3}R\right) \tag{31}$$

$$\Lambda_1 = \left(2EcPrS\left(\frac{A_2}{A_3}\right)\left((1-\phi)+\phi\frac{\rho_{CNT}}{\rho_f}\right)(1-\phi)^{-2.5}\frac{d\upsilon_0}{dx}\frac{d\upsilon_1}{dx}+4\delta EcPr\left(\frac{1}{A_3}\right)\left(\frac{d\upsilon_0}{dx}\right)^3\frac{d\upsilon_1}{dx}\right)/\left(1+\frac{4}{3}R\right) \tag{32}$$

Zeroth order solution can be obtained by simplifying the recursive relation Eqs. (23) -(24) using the leading order boundary condition Eq. (25) which yields.

$$\upsilon_0 = \frac{x^3}{4}-\frac{x}{4} \tag{33}$$

$$\theta_0 = -\frac{x}{2} \tag{34}$$

First order solution can be obtained from Eqs.(29) and (31) which is expressed as

$$\upsilon_1 = L_{xx}^{-1}(\Gamma_0) \tag{35}$$

$$\theta_1 = L_{xx}^{-1}(\Lambda_0) \tag{36}$$

with the first order boundary condition as follows

$$\upsilon_1 = 0, \theta_1 = 0.5 \text{ at } x = -1$$
$$\upsilon_1 = 0, \theta_1 = -0.5 \text{ at } x = 1 \tag{37}$$

Upon simplifying Eqs. (35) and (36) with the aid of first order boundary condition Eq. (37).This can be easily shown as

$$\upsilon_1 = 6\delta SA_1\left((1-\phi)+\phi\frac{\rho_{CNT}}{\rho_f}\right)(1-\phi)^{2.5}\left(\frac{9x^5}{80}-\frac{3x^3}{48}+\frac{x}{160}\right) \tag{38}$$

$$\theta_1 = \left(\begin{array}{l} EcPrS\left(\frac{A_2}{A_3}\right)\left((1-\phi)+\phi\frac{\rho_{CNT}}{\rho_f}\right)(1-\phi)^{-2.5}\left(\frac{9x^6}{480}-\frac{3x^4}{96}+\frac{x^2}{32}+\frac{9x}{160}-\frac{3}{40}\right) \\ +2\delta EcPr\left(\frac{1}{A_3}\right)^*\left(\frac{81x^{10}}{23040}-\frac{27x^8}{3584}+\frac{27x^6}{3840}-\frac{3x^4}{768}+\frac{x^2}{512}+\frac{57x}{17920}-\frac{19}{4480}\right)\end{array}\right)/\left(1+\frac{4}{3}R\right) \tag{39}$$

Second order solution can be obtained from Eqs.(30) and (32) which is expressed as

$$\upsilon_2 = L_{xx}^{-1}(\Gamma_1) \tag{40}$$

$$\theta_2 = L_{xx}^{-1}(\Lambda_1) \tag{41}$$

with the second order boundary condition as follows

$$\upsilon_2 = 0, \theta_2 = 0.5 \text{ at } x = -1$$
$$\upsilon_2 = 0, \theta_2 = -0.5 \text{ at } x = 1 \tag{42}$$

Upon simplifying Eqs. (40) and (41) with the aid of second order boundary condition Eq. (42) can be easily shown as

Table 2. Validations of temperature profiles across varying X values. When Pr = Ec = δ = S = 1, ϕ = R = 0.

X	θ(X)			Error	Error
	NS [8]	HPM [8]	ADM	HPM	ADM
-1.0000	0.5000	0.5000	0.5000	0.0000	0.0000
-0.8000	0.4007	0.4007	0.4007	0.0000	0.0000
-0.6000	0.3011	0.3012	0.3012	0.0001	0.0001
-0.4000	0.2015	0.2016	0.2015	0.0001	0.0000
-0.2000	0.1018	0.1019	0.1017	0.0001	0.0001
0.20000	-0.0981	-0.0981	-0.0980	0.0000	0.0000
0.40000	-0.1984	-0.1984	-0.1984	0.0000	0.0000
0.60000	-0.2989	-0.2988	-0.2989	0.0001	0.0000
0.80000	-0.3993	-0.3993	-0.3994	0.0000	0.0001
1.00000	-0.5000	-0.5000	-0.5000	0.0000	0.0000

Table 3. Effect of MWCNT'S and radiation on the thermal profile. When Pr = Ec = δ = 1, ϕ = 0.05 and R = 5.

X at (S=1)	ϴ (X)	X at (S= -1)	ϴ (X)
-1.0000	-0.4190	-1.0000	1.2529
-0.8000	-0.5387	-0.8000	1.1934
-0.6000	-0.6227	-0.6000	1.0996
-0.4000	-0.6983	-0.4000	0.9953
-0.2000	-0.7640	-0.2000	0.8810
0.00000	-0.8124	0.00000	0.7518
0.2000	-0.8400	0.2000	0.6054
0.4000	-0.8503	0.4000	0.4441
0.6000	-0.8508	0.6000	0.2727
0.8000	-0.8428	0.8000	0.0909
1.0000	-0.7992	1.0000	-0.1252

$$\upsilon_2 = 6\delta S \frac{A_1}{A_4}\left|(1-\phi)+\phi\frac{\rho_{CNT}}{\rho_f}\right|(1-\phi)^{2.5}\left(\frac{135x^9}{18432}-\frac{183x^7}{10752}+\frac{329x^5}{25600}-\frac{33x^3}{7680}+\frac{57x}{50000}\right) \tag{43}$$

$$\theta_2 = \left|\begin{matrix} 2EcPrS\left(\dfrac{A_2}{A_3}\right)\left|(1-\phi)+\phi\dfrac{\rho_{CNT}}{\rho_f}\right|(1-\phi)^{-2.5}\left(\dfrac{15x^8}{7168}-\dfrac{13x^6}{3840}+\dfrac{33x^4}{7680}+\dfrac{x^2}{1280}+\dfrac{567x}{50000}-\dfrac{189}{12500}\right)+ \\ 4\delta EcPr\left(\dfrac{1}{A_3}\right)^{*}\left(\dfrac{135x^{12}}{270336}-\dfrac{297x^{10}}{184320}+\dfrac{531x^8}{286720}-\dfrac{161x^6}{153600}+\dfrac{9x^4}{122880}+\dfrac{9x}{12500}-\dfrac{3}{3125}\right) \end{matrix}\right| \Big/ \left(1+\frac{4}{3}R\right) \tag{44}$$

The summations of Eqs. (33),(38) and (43) gives the ADM solutions for the velocity profile while Eqs. (34),(39) and (44) gives the solution for temperature profile. Which is expressed as

$$\begin{aligned}\upsilon = {} & \frac{x^3}{4}-\frac{x}{4}+6\delta SA_1\left|(1-\phi)+\phi\frac{\rho_{CNT}}{\rho_f}\right|(1-\phi)^{2.5}\left(\frac{9x^5}{80}-\frac{3x^3}{48}+\frac{x}{160}\right)+6\delta SA_1\left|(1-\phi)+\phi\frac{\rho_{CNT}}{\rho_f}\right| \\ & (1-\phi)^{2.5}\left(\frac{135x^9}{18432}-\frac{183x^7}{10752}+\frac{329x^5}{25600}-\frac{33x^3}{7680}+\frac{57x}{50000}\right)\end{aligned} \tag{45}$$

$$\theta = -\frac{x}{2}+\left|\begin{matrix} EcPrS\left(\dfrac{A_2}{A_3}\right)\left|(1-\phi)+\phi\dfrac{\rho_{nf}}{\rho_f}\right|(1-\phi)^{-2.5}\left(\dfrac{9x^6}{480}-\dfrac{3x^4}{96}+\dfrac{x^2}{32}+\dfrac{9x}{160}-\dfrac{3}{40}\right)+2\delta EcPr\left(\dfrac{1}{A_3}\right)^{*} \\ \left(\dfrac{81x^{10}}{23040}-\dfrac{27x^8}{3584}+\dfrac{27x^6}{3840}-\dfrac{3x^4}{768}+\dfrac{x^2}{512}+\dfrac{57x}{17920}-\dfrac{19}{4480}\right)+2EcPrS\left(\dfrac{A_2}{A_3}\right)\left|(1-\phi)+\phi\dfrac{\rho_{nf}}{\rho_f}\right|(1-\phi)^{-2.5} \\ \left(\dfrac{15x^8}{7168}-\dfrac{13x^6}{3840}+\dfrac{33x^4}{7680}+\dfrac{x^2}{1280}+\dfrac{567x}{50000}-\dfrac{189}{12500}\right)+4\delta EcPr\left(\dfrac{1}{A_3}\right)^{*}\left(\begin{matrix}\dfrac{135x^{12}}{270336}-\dfrac{297x^{10}}{184320}+\dfrac{531x^8}{286720}-\dfrac{161x^6}{153600}+ \\ \dfrac{9x^4}{122880}+\dfrac{9x}{12500}-\dfrac{3}{3125}\end{matrix}\right) \end{matrix}\right| \Big/ \left(1+\frac{4}{3}R\right) \tag{46}$$

3. Results and Discussion

This section discusses the results obtained from the analytical solution for the thermal radiating film flow of sodium alginate conveying the multi walled carbon nanoparticles through flat plates. The pertinent parameters are fixed for all cases at Pr= Ec=0.1, δ=0.5, S=1, ϕ=0.01 and R=1 unless stated otherwise. The natural convecting flowing fluid was examined using the adomian method of analytical approximate solution. This was confirmed for correctness against the numerical Runge Kutta fourth order method (RK-4) and the analytical homotopy perturbation method (HPM), this is shown in the Table 2, which shows the absolute error of the ADM and HPM analytical methods against the numerical RK-4 method. The Table 3, reveals the effect of MWCNT nanoparticles and radiation effect on the fluid transport. It is observed that heat transfer rate increases due to enhanced kinematic viscosity and thermal conductivity of fluid. As shown in the Table 3 as plate moves together (S=-1) the thermal profile decreases while as plate recedes thermal profile further decreases as rapid heat exchange leads to thermal loss. Results reveals concentration of the multi walled nanoparticles reduces the flow of the fluid owing to the decrease in the thickness of momentum boundary layer which impedes flow velocity, this is observed in Fig.2. The squeezing effect of the plates on the fluid transport reveals a converse report. As the plates constrict (S<0) the velocity slightly increases and as plate recedes (S<0) rapid increase is observed at the left wall. The transport velocity decrease is seen near the right walls which connotes constant mass flow rate which increases gradient of velocity. Ultimately increased velocity of fluid at mid plate will compensate for decreased flow near region of wall. However, the situation at the left wall is due to backflow as a result of decreased kinematic viscosity.

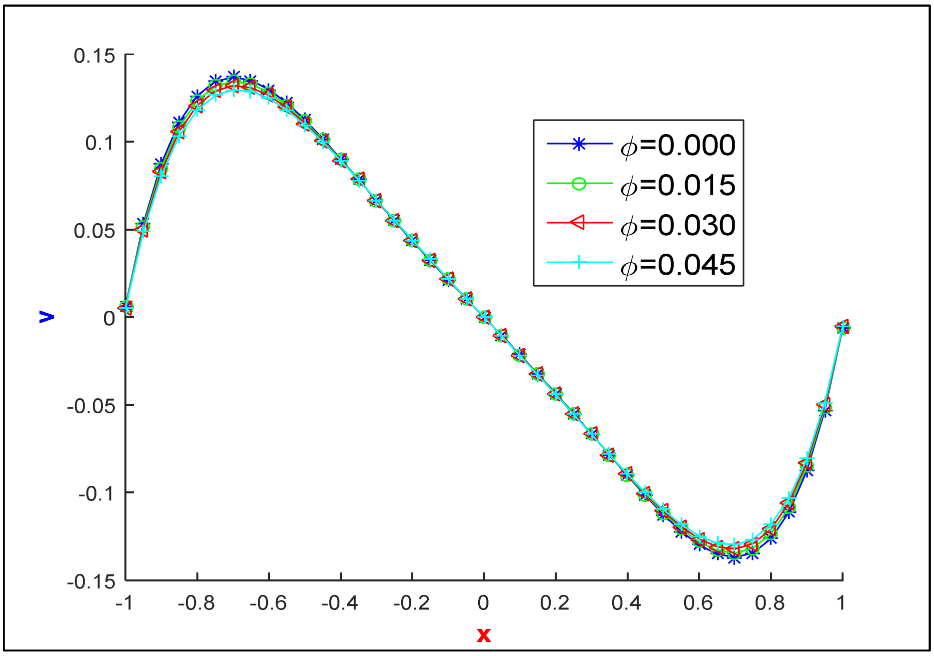

Fig. 2. Nanoparticles concentration effect on velocity profile utilizing MWCNT.

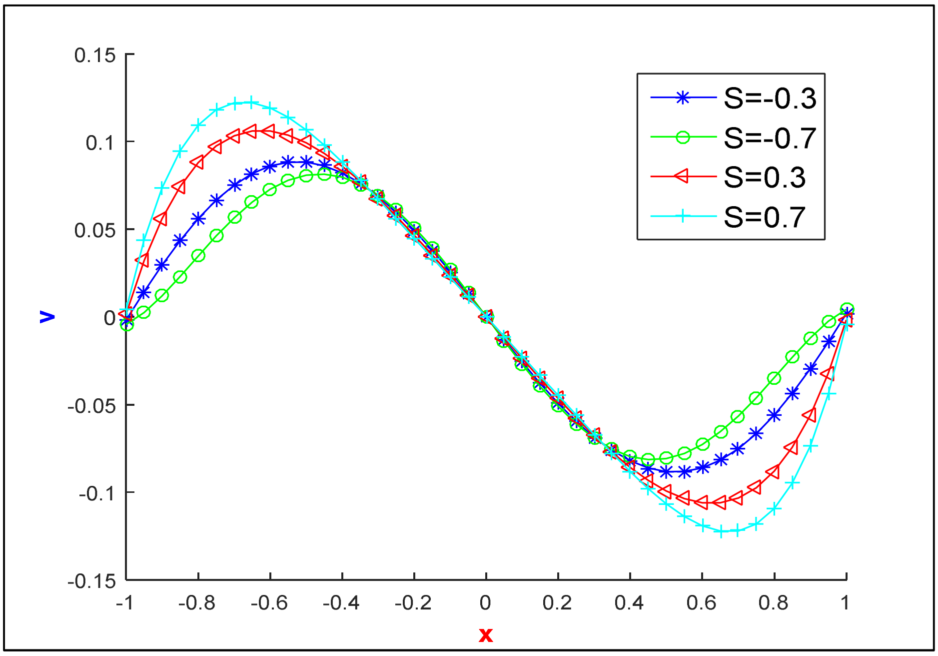

Fig. 3. Squeezing parameter effect on velocity profile utilizing MWCNT.

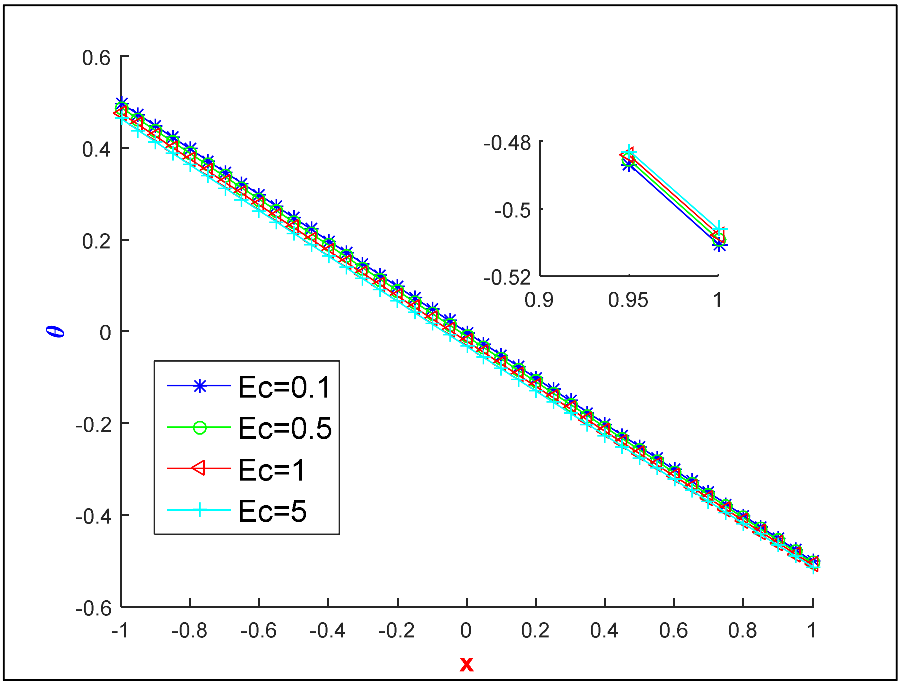

Fig. 4. Eckert parameter effect on thermal profile utilizing MWCNT.

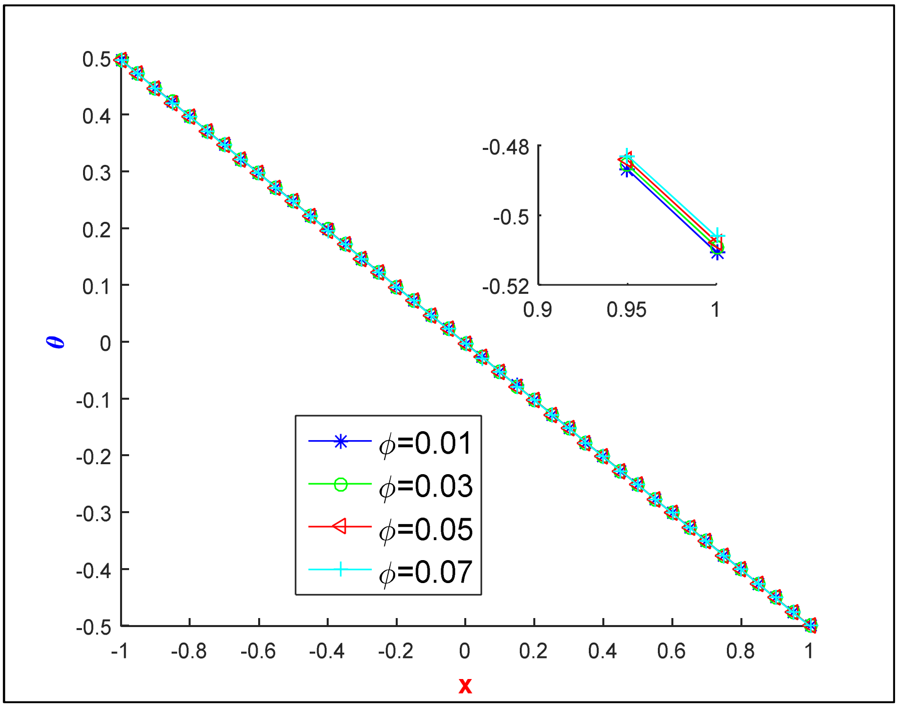

Fig. 5. Nanoparticles concentration effect on thermal profile utilizing MWCNT.

Frictional heating enhances by fluid velocity owing to viscous dissipation effect enhances the thickness of the thermal boundary layer thickness. This leads to the increase of the Eckert parameter effect on thermal distribution of Sodium alginate radiating flow which causes thermal profile decrease. However, the thermal decrease towards the left plate is higher than the right plate this is observed in Fig. 4. As revealed from thermal profile Fig. 5, concentration increase of MWCNT nanoparticles increases thermal profile significantly. This can be explained physically owing to increasing concentration, increases thickness of thermal boundary due to conductivity enhancement of fluid. Improved thermal diffusivity drops thermal gradient which reduces heat transfer. The Prandtl's number effect on the heat transfer is reported in Fig.6, increasing Prandtl's number depicts dominant boundary layer momentum compared to the thermal boundary layer. This depicts thermal diffusivity is recessive against fluid kinematic viscosity owing to force balance in thermal boundary layer buoyancy and viscosity consequently decrease in thermal profile is observed. The thermal radiating film effect on the nanofluid flow is investigated in Fig. 7, increasing radiation parameter during fluid transport enhances heat dissipation which subsequently leads to thermal drop which decreases thickness of thermal boundary. Moreso radiation effect on the physical parameter of the heat transfer is observed in Fig. 8, Nusselt number reveals quantitative decrease of the radiation parameter causes decrease in heat transfer as plates rescind while as plates constrict higher values of heat transfer is noticed.

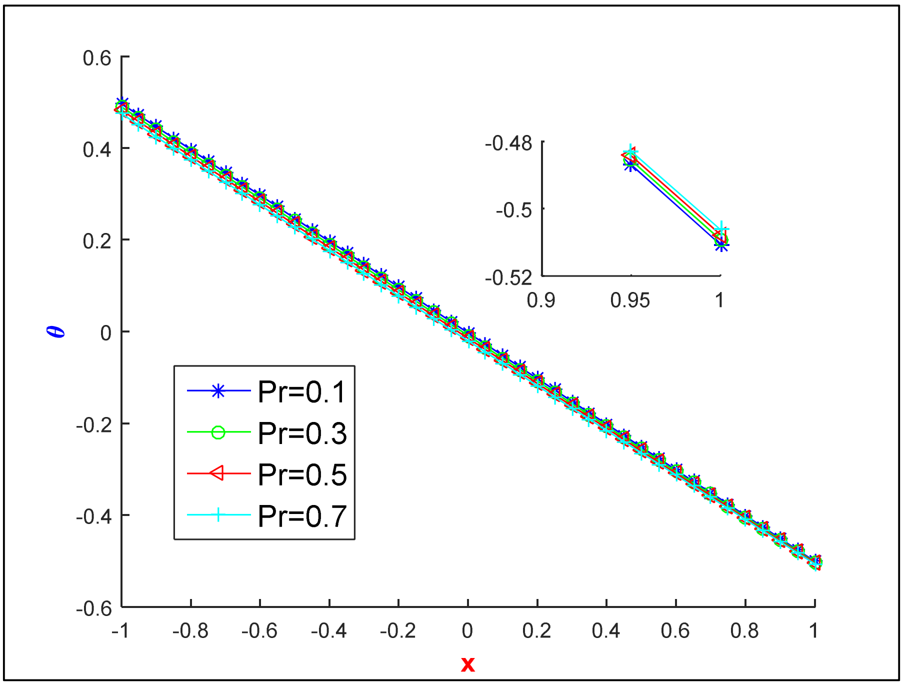

Fig. 6. Prandtl number effect on thermal profile utilizing MWCNT.

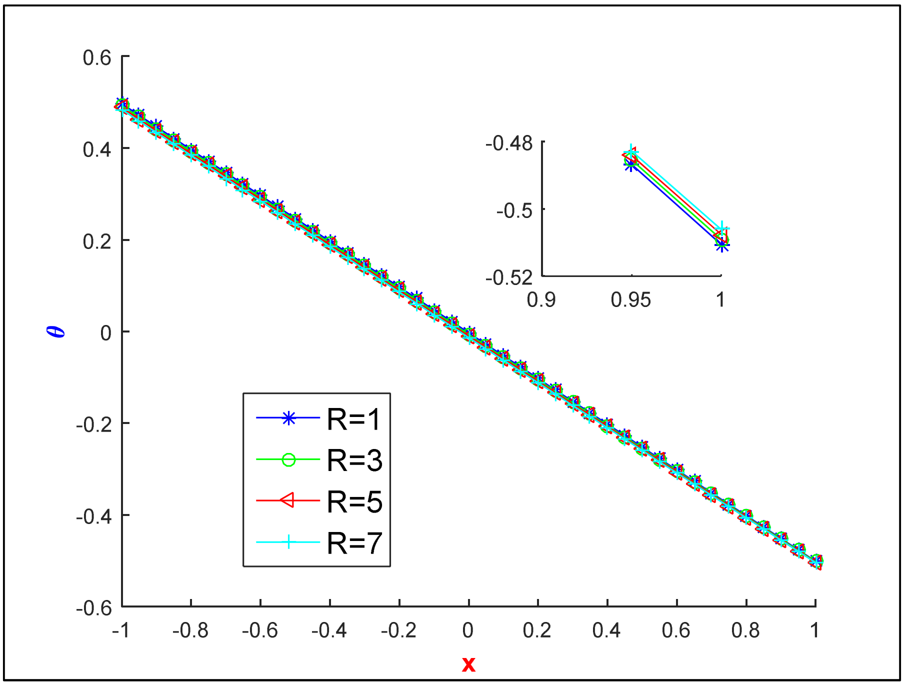

Fig. 7. Radiation parameter effect on thermal profile utilizing MWCNT.

4. Conclusion

The effect of thermal squeezing flow with multi-walled carbon nanotube nanoparticle is investigated in this paper, considering radiation. The base fluid of sodium alginate, a non-Newtonian fluid was examined using a system of nonlinear ordinary equations. This was decomposed and solved using the adomian decomposition method. The result obtained was validated against fourth order Runge kutta and homotopy perturbation method of solution for the correctness which gives similar results. Consequently, this renews confidence. As observed, radiation effect on fluid transport shows decrease in heat transfer as thermal conductivity becomes lower than temperature gradient of the flow. While the concentration increase of nanoparticles improves thickness of thermal boundary due to conductivity enhancement of fluid which drops thermal gradient reducing heat transfer. Therefore, the results obtained from the work provides a good basis for applications of the Sodium alginate including include in medical, pharmaceutical and manufacturing industries. It is therefore recommended that further studies will be conducted for the sodium alginate transport utilizing extended transport channels and improved geometry shape nanoparticles.

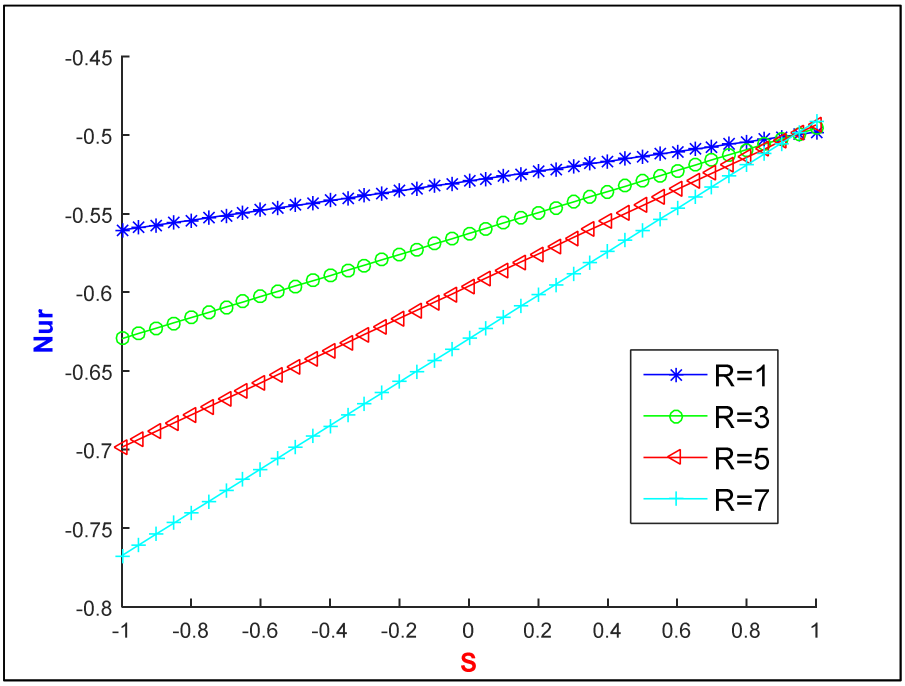

Fig. 8. Squeezing and radiation parameter effect on the Nusselt number utilizing MWCNT.

Author's Contribution

A.T. Akinshilo formulated the model, analyzed the problem, simulated and generated the results, A. Davodi validated the result, A. Ilegbusi wrote the manuscript and G. Sobamowo proposed the problem and directed the research.

Acknowledgement

The authors express their profound gratitude to Mrs. Abimbola E. Akinshilo, who painstakingly proof read and typeset the manuscript within short period of notification for grammatical correctness.

Conflict of Interest

The authors declared no potential conflicts of interest with respect to the research, authorship, and publication of this article.

Funding

The authors received no financial support for the research, authorship, and publication of this article.

Data Availability Statements

The datasets generated and/or analyzed during the current study are available from the corresponding author on reasonable request.

Nomenclature

E_c	Eckert number	Greek symbols	
g	Acceleration due to gravity	α	Thermal diffusivity
G	Material constant	σ	Electrical conductivity
k	Thermal conductivity	β_3	Activation energy parameter
k_f	Base fluid thermal conductivity	δ	Dimensionless non-Newtonian parameter
k_{nf}	Effective thermal conductivity	ε	Dimensionless thermal conductivity parameter
k_s	Nanoparticle thermal conductivity	μ_{nf}	Effective dynamic viscosity
P_r	Prandtl number	θ	Dimensionless Temperature
R	Radiation parameter	$(\rho C_p)_f$	Base fluid heat capacity
S	Squeeze parameter	$(\rho C_p)_{nf}$	Effective heat capacity
T	Initial temperature	$(\rho C_p)_s$	Nanoparticle heat capacity
T_m	Mean temperature	ρ_f	Base fluid density
v	Velocity in x Direction	ρ_{nf}	Effective density
V	Dimensionless velocity in x direction	ρ_s	Nanoparticle density
R	Dimensionless Radiation parameter	υ	Kinematic viscosity

References

[1] Hosseinzadeh, Kh., Alizadeh, M., Ganji, D.D., Hydrothermal analysis on MHD squeezing nanofluid flow in parallel plates by analytical method, *International Journal of Mechanical and Materials Engineering*, 143, 2020, 39-52.
[2] Ziabakhsh, Z., Domairry, G., Analytic solution of natural convection flow of a non-Newtonian fluid between two vertical flat plates using homotopy analysis method, *Communication Nonlinear Science and Numerical Simulation*, 14, 2009, 1868-1880.
[3] Mustafa, M., Hayat, T., Obadiat, S., On heat and mass transfer in an unsteady squeezing flow between parallel plates, *Mechanica*, 47, 2012, 1581-1589.
[4] Jaiyesimi, L.O., Sobamowo, M.G., Akinshilo, A.T., Waheed, M.A., Chebychev spectral collocation method to micropolar fluid flow through a porous channel driven with high mass transfer, *World Scientific News; an International Journal*, 143, 2020, 39-52.
[5] Adesanya, S.O., Falade, J.A., Thermodynamic analysis of hydro magnetic third grade fluid flow through a channel filled with porous medium, *Alexandria Engineering Journal*, 14, 2015, 615-622.
[6] Hoshyar, H.A., Ganji, D.D., Borranc, A.R., Falahatid, M., Flow behavior of unsteady incompressible Newtonian fluid flow between two parallel plates via homotopy analysis method, *Latin American Journal of Solids and structures*, 12, 2015, 1859-1869.
[7] Ijaz, N., Zeeshan, A., Bhatti, M.M., Ellahi, R., Analytical study on liquid solid particles interaction in the presence of heat and mass transfer through a wavy channel, *Journal of Molecular Liquids*, 250, 2018, 80-87.
[8] Kargar, A., Akbarzade, M., Analytical solution of Natural convection Flow of a non-Newtonian between two vertical parallel plates using the Homotopy Perturbation Method, *World Applied Sciences Journal*, 20, 2012, 1459-1465.
[9] Turkyilmazoglu,M., Condensation of lamina film flow over a curved vertical wall using single- and two-phase nano fluid models, *European Journal of Mechanics-B/Fluids*, 65, 2017, 184-191.
[10] Hatami, M. Ganji, D.D., Natural convection of sodium alginate (SA) non-Newtonian nanofluid flow between two vertical flat plates by analytical and numerical methods, *Thermal Engineering*, 2, 2014, 14-22.
[11] Hatami, M., Hatami, J., Jafayar, M., Domairry, G., Differential transformation method for Newtonian and non-Newtonian fluid analysis: Comparison with HPM and numerical solution, *Journal of Brazilian Society of Mechanical Science and Engineering*, 38, 2016, 589-599.
[12] Ahmadi, A.R., Zahmatkesh, A., Hatami, M., Ganji, D.D., Comprehensive analysis of the flow and heat transfer for nanofluid over an unsteady stretching flat plate, *Powder Technology*, 258, 2014, 125-133.
[13] Ghadhikolaei, S.S., Hosseinzadeh, K, Ganji, D.D., Analysis of unsteady MHD Eyring Powel squeezing flow in stretching channel with considering thermal radiation and joule heating effect using AGM, *Case Studies in Thermal Engineering*, 10, 2017, 579-594.
[14] Sheikholeslami, M., Rashidi, M.M., Alsaad, D.M., Rokni, H.B., Steady nanofluid flow between parallel plates considering thermophoresis and Brownian effects, *Journal of King Saud University Science*, 28(4), 2016, 380-389.
[15] Pourmehran, O., Rahimi-Gorji, M., Gorji-Bandpy, M., Ganji, D.D., Analytical investigation of squeezing unsteady nanofluid flow between parallel plates by LSM and CM, *Alexandria Engineering Journal*, 54, 2015, 17-26.
[16] Ghadikholaei, S.S., Hosseinzadeh, K., Yassari,M., Sadeghi, H., Ganji, D.D., Boundary layer analysis of micropolar dusting fluid with TiO_2 nanoparticles in a porous medium under the effect magnetic field and thermal radiation over a stretching sheet, *Journal of Molecular Liquids*, 244, 2017, 374-389.
[17] Ghadikholaei, S.S., Yassari, M., Sadeghi, H.,Hosseinzadeh, K, Ganji, D.D., Investigation on thermophysical properties of TiO2-Cu /H2O hybrid nanofluid transport dependent on shape factor in MHD stagnation point flow, *Powder Technology*, 322, 2017, 428-438.
[18] Domairry, G., Hatami, M., Squeezing Cu-water nanofluid flow analysis between parallel plates by DTM-Pade Method, *Journal of Molecular Liquids*, 188, 2014, 155-161.
[19] Afify, A.A., Abdel-Azizi, M., Lie group analysis of flow and heat transfer of non-Newtonian nanofluid, *Pramana Journal of Physics*, 31, 2017, 88-104.
[20] Sheikholeslami, M., Abelman, S., Two phase simulation of nanofluid flow and heat transfer in an annulus in the presence of an axial magnetic field, *IEEE Transaction on Nanotechnology*, 14, 2015, 561-566.
[21] Madaki, A.G., Roslan, R., Mohamed, M., Kamardan, M.G., Analytical solutions of squeezing unsteady nanofluid flow in the presence of thermal radiation, *Journal of Computer Science and Computational Mathematics*, 6, 2016, 451-463.
[22] Akinshilo, A.T., Olofinkua, J.O., Olaye, O., Flow and Heat Transfer Analysis of Sodium Alginate Conveying Copper Nanoparticles between Two Parallel Plates, *Journal of Applied and Computational Mechanics*, 3(4), 2017, 25-266.
[23] Menni, Y., Azzi, A., Chanmkha, A.J., A review of solar energy collector: models and applications, *Journal of Applied and Computational Mechanics*, 4(4), 2018, 375-401.
[24] Menni, Y., Azzi, Chamkha, A.J., Harmand, S., Analysis of fluid dynamics and heat transfer in a rectangular duct with staggered baffles, *Journal of Applied and Computational Mechanics*, 5(5), 2019, 231-248.
[25] Menni, Y., Azzi, Chamkha, A.J., The solar air channels: comparative analysis, introduction of arc shaped fins to improve thermal transfer, *Journal of Applied and Computational Mechanics*, 5(4), 2019, 616-626.
[26] Menni, Y., Chamkha, A.J., Azzi, Y., Fluid flow and heat transfer over staggered "+" shaped obstacles, *Journal of Applied and Computational Mechanics*, 2018, doi.10.22055/JACM.2018.2677.1316.
[27] Menni, Y., Chamkha, A.J., Ahmadi, M.H., Hydrodynamic behavior in solar oil heat exchanger ducts fitted with staggered baffles and fins, *Journal of Applied and Computational Mechanics*, 2020, doi.10.22055/JACM.2020.32468.2021.
[28] Chamkha, A.J., Menni, Y., Ameur, H., Thermal aerodynamic performance measurement of air heat transfer fluid mechanics over s-shaped fins in shell and tube heat exchangers, *Journal of Applied and Computational Mechanics*, 2020, doi.10.22055/JACM.2020.32107.1970.
[29] Sakhri, N., Menni, Y., Chamkha, A.J., Heating capacity of an earth to air heat exchanger in arid regions- experimental investigation, *Journal of Applied and Computational Mechanics*, 2020, doi.10.22055/JACM.2020.31237.1843.
[30] Kaseian, A., Daneshazarian, R., Mahian, O., Kolsi, A.J., Chamkha, A.J., Wongwises, S., Nanofluid transport in porous media- a review of the latest development, *International Journal of Heat and Mass Transfer*, 107, 2017, 778-791.
[31] Menni, Y., Chamkha, A.J., Ahmed, A., Nanofluid flow in complex geometries- a review, *Journal of Nanofluid*, 8(5), 2019, 893-916.
[32] Menni, Y., Chamkha, A.J., Lorenzini, G., Noueddine, K., Ameur, H., Nensafi, M., Advances of nanofluid flow in solar collectors- A review of numerical studies, *Mathematical Modelling of Engineering Problem*, 060313, 2019, 415-427.
[33] Menni, Y., Chamkha, A.J., Massarotti, N., Ameur, H., Kaid, N., Bensafi, M., Hydrodynamics and thermal analysis of water, ethylene glycol, and water-ethylene glycol as base fluids dispersed by aluminum nano-sized solid particles, *International Journal of Numerical Methods for Heat and Fluid Flow*, 2019, doi.10.11081/HFF-10-2019-0739.

[34] Menni, Y., Zidani, A.J., Benyoucef, C., Heat and nanofluid transfer through baffled channel in different outlet models, *Mathematical Modelling of Engineering Problem*, 6(1), 2019, 52-60.
[35] Menni, Y., Chamkha, A.J., Ahmed, A., Numerical analysis of heat transfer and nanofluid mass transfer in a channel with detached and attached baffled plates, *Journals of Nanofluids*, 8(5), 2019, 83-916.
[36] Choi, S.U.S., Engineering thermal conductivity of fluids with nanoparticles, *Development and Application of Non-Newtonian Flows*, 66, 1995, 99-105.
[37] Alizadeh, M., Dogonchi, A.S., Ganji, D.D., Micropolar nanofluid flow and heat transfer between penetrable walls by the presence of thermal radiation and magnetic field, *Case Studies in Thermal Engineering*, 12, 2018, 319-322.
[38] Dogonchi, A.S., Ganji, D.D., Impact of Cattaneo-Christov heat flux on MHD nanofluid flow and heat transfer between parallel plate considering thermal radiation effect, *Journal Institution of Chemical Engineers*, 80, 2017, 52-63.
[39] Akinshilo, A.T., Investigation of nanofluid conveying porous medium through non-parallel plates using the Akbari Ganji method, *Physica Scripta*, 2019, http://doi.org/10.1088/1402-4896/ab52f6.
[40] Hayat, T., Nasir, T., Khan, M.I, Alsaedi, A., Non-Darcy flow of water based single (SWCNTS) and multiple (MWCNTS) walls carbon nanotubes with multiple slip condition due to rotating disk, *Results in Physics*, 9, 2019, 390-399.
[41] Yan, S.R., Kalbasi, R., Nguyen, Q., Karimipour, A., Sensitivity of adhesive and cohesive intermolecular forces to the incorporation of MWCNTs into liquid paraffin: Experimental study and modelling of surface tension, *Journal of Molecular Liquids*, 310, 2020, 113235.
[42] Tian, Z, Rostamis, S., Taherialekouhi, R., Karimipour, A., Moradikazerouni, A., Yarmand, H., Zulkifli, N.W.B.M., Prediction of rheological behavior of a new hybrid nanofluid consists of copper oxide and multi walled carbon nanotubes suspended in a mixture of water and ethylene glycol using curve fitting on experimental data, *Physica A: Statistical Mechanics and Its Applications*, 549, 2020, 124101.
[43] Sharifzadeh, B., Kalbasi, R., Jahangiri, M., Toghraie, D., Karimipour, A., Computer modelling of pulsatie blood flow in elastic artery using a software program for application in biomedical engineering, *Computer Methods and Programs in Biomedicine*, 192, 2020, 105442.
[44] Farzinpour, M., Toghraie, D., Mehmandoust, B., Aghadavoudi, F., Karimipour, A., Molecular dynamics study of barrier effects on ferro-nanofluid flow in the presence of constant and time dependent external magnetic field, *Journal of Molecular Liquids*, 308, 2020, 113152.
[45] Yan, S.R., Kalbasi, R., Nguyen, Q., Karimpour, A., Rheological behavior of hybrid MWCNTs-TiO_2/EG nanofluid: A comprehensive modelling and experimental study, *Journal of Molecular* Liquids, 306, 2020, 112937.
[46] Yan, S.R., Shirani, A., Zarringhalam, M., Nguyen, Q., Karimipour, A., Prediction of boiling flow characteristics in rough and smooth microchannels using molecular dtnamics simulatin: Investigation the effects of boundary wall temperatures, *Journal of Molecular Liquids*, 308, 2020, 113058.
[47] Filobello-Niño, U., Vazquez-Leal, H., Boubaker, K., Khan, Y., Perez-Sesma, A., Sarmiento Reyes, A., Jimenez-Fernandez, V.M., Diaz-Sanchez, A. Herrera-May, A., Sanchez-Orea, J., Pereyra-Castro, K., Perturbation Method as a Powerful Tool to Solve Highly Nonlinear Problems: The Case of Gelfand's Equation, *Asian Journal of Mathematics and Statistics*, 6, 2013, 76-82.
[48] Bhatti, M.M., Rashidi, M.M., Pop, I., Entropy generation with nonlinear heat and mass transfer on MHD boundary layer over a moving surface using SLM, *Nonlinear Engineering*, 6, 2017, 43-52.
[49] Akinshilo, A.T., Olaye, O., On the analysis of the Erying Powell model based fluid flow in a pipe with temperature dependent viscosities and internal heat generation, *Journal of King Saud-Engineering Sciences*, 31, 2019, 271-279.
[50] Hassan, W., Sajjad, H., Humaira, S., Shanila, K., MHD forced convection flow past a moving boundary surface with prescribed heat flux and radiation, *British Journal of Mathematics and Computer Science*, 21, 2017, 1-14.
[51] Bank, R.N., Dash, G.C., Chemical reaction effect on peristaltic motion of micropolar fluid through a porous medium with heat absorption the presence of magnetic field, *Advances in Applied Science Research*, 6, 2015, 20-34.
[52] Mekonnen, S.A., Negussie, T.D., Hall effect and temperature distribution on unsteady micropolar fluid flow in a moving wall, *International Journal of Science Basic and Applied Research*, 24, 2015, 60-75.
[53] Mekheir, K.S., Mohammed, S.M., Interaction of pulsatile flow on peristaltic motion of magneto micropolar fluid through porous medium in a flexible channel: Blood flow model, *International Journal Pure and Applied Mathematics*, 94, 2014, 323-339.
[54] Pour, M., Nassab, S., Numerical investigation of forced laminar convection flow of nanofluid over a backward facing step under bleeding condition, *Journal of Mechanics*, 28(2), 2012, 7-12.
[55] Hatami, M., Jing, D., Differential transformation method for Newtonian and non-Newtonian nanofluid flow analysis: compared to numerical solution, *Alexander Engineering Journal*, 55, 2016, 731-739.
[56] Trkyilmazoglu, M., Mixed convection of magnetohydramic micropolar due to a porous heater / heated deformable plate: exact solution, *International Journal Heat Mass Transfer*, 2017, 127-134.
[57] Akinshilo, A.T., Flow and heat transfer of nanofluid with injection through an expanding or contracting porous channel under magnetic force field, *Engineering Science and Technology, an International Journal*, 21, 2018, 486-494.
[58] Chamkha, A.J., Molana, M., Rahnama, A., Ghadami, F., On the nanofluids applications in microchannels: a comprehensive review, *Powder Technology*, 332(1), 2018, 287-322.
[59] Chamkha, A.J., Solar radiation assisted natural convection in uniform porous medium supported by a vertical flat plate, *Journal of Heat Transfer*, 11991, 1997, 89-96.
[60] Damseh, R.A., Al-Odat, M.Q., Chamkha, A.J., , Shannak, B.A., Combined effect of heat generation or absorption and first-order chemical reaction on micropolar fluid flows over a uniformly stretched permeable surface: The full analytical solution, *International Journal of Thermal Science*, 48(8), 2009, 1658-1663.
[61] Chamkha, A.J., Takhari, H.S., Soundalgekar, V.M., Radiation effects on free convection flow past a semi-infinite vertical plate with mass transfer, *Chemical Engineering Journal*, 8(3), 2001, 335-344.
[62] Umvathi, J.C., Chamkha, A.J., Mateen, A., Al-Mudhaf, A., Unsteady two-fluid flow and heat transfer in a horizontal channel, *Heat and Mass Transfer*, 42, 2005, 81.
[63] Chamkha, A.J., Rashad, A.M., Mansour, M.A., Armaghani, T., Ghalambaz, M., Effects of heat sink and source and entropy generation on MHD mixed convection of a Cu-water nanofluid in a lid-driven square porous enclosure with partial slip, *Physics of Fluid*, 29, 2017, 052001.
[64] Rashad, A., Armaghani, T., Chamkha, A.J., Mansour, M.A., Entropy generation and MHD natural convection of a nanofluid in an inclined square porous cavity: effects of a heat sink and source size and location, *Chinese Journal of Physics*, 56(1), 2018, 193-211.
[65] Parvin, S., Nasrin, R., Alim, A., Hossain, N.K., Chamkha, A.J., Thermal conductivity variation on natural convection flow of water–alumina nanofluid in an annulus, *International Journal of Heat and Mass Transfer*, 55(19), 2012, 5268-5274.

[66] Chamkha, A.J., Flow of two-immiscible fluids in porous and nonporous channels, *Journal of Fluid Engineering*, 122(1), 2000, 117-124.
[67] Khanafer, K.M., Chamkha, A.J., Hydromagnetic natural convection from an inclined porous square enclosure with heat generation, *An International Journal of Computation and Methodology*, 33(8), 199, 81-910.
[68] Chamkha, A., Ismael, M., Kasaeipoor, A., Armaghani, T., Entropy generation and natural convection of CuO-water nanofluid in C-shaped cavity under magnetic field, *Entropy*, 18, 2016, 50.
[69] Chamkha, A.J., Boostanidezfuli, A., Izadpanahi, E., Ghalambaz, M., Phase-change heat transfer of single/hybrid nanoparticles-enhanced phase-change materials over a heated horizontal cylinder confined in a square cavity, *Advanced Powder Technology*, 28(2), 2017, 385-397.
[70] Takhar, H.S., Chamkha, A.J., Nath, G., Unsteady three-dimensional MHD-boundary-layer flow due to the impulsive motion of a stretching surface, *Acta Mechanica*, 146, 2001, 59-71.
[71] Chamkha, A.J., Khalid, A.A., Hydromagnetic Natural Convection from an Isothermal Inclined Surface Adjacent to a Thermally Stratified Porous Medium, *International Journal of Numerical Method for Heat and Fluid Flow*, 10(5), 2000, 455-477.
[72] Chamkha, A.J., Khaled, A.A., Hydromagnetic combined heat and mass transfer by natural convection from a permeable surface embedded in a fluid-saturated porous medium, *International Journal of Numerical Methods For Heat and Fluid Flow*, 10(5), 2000, 455-477.
[73] Zakari, A., Ghalambaz, M., Chamkha, A.J., Rossi, D.D., Theoretical analysis of natural convection boundary layer heat and mass transfer of nanofluids: effects of size, shape and type of nanoparticles, type of base fluid and working temperature, *Advanced Powder Technology*, 26(3), 2015, 935-946.
[74] Chamkha, A.J., Al-Mudhaf, A., Unsteady heat and mass transfer from a rotating vertical cone with a magnetic field and heat generation or absorption effects, *International Journal of Thermal Science*, 44(3), 2005, 267-276.
[75] Chamkha, A.J., Issa, C., Effect of Heat Generation or Absorption on Thermophoretic Free Convection Boundary Layer From a Vertical Flat Plate Embedded in a Porous Medium, *International Journal of Numerical Methods for Heat and Fluid Flow*, 10(4), 2000, 432-449.
[76] Ghalambaz, M., Behseresht, A., Behseresht, J., Chamkha, A.J., Effects of nanoparticles diameter and concentration on natural convection of the Al2O3–water nanofluids considering variable thermal conductivity around a vertical cone in porous media, *Advanced Powder Technology*, 26(1), 2015, 224-235.
[77] Subba, R., Gorla, R., Chamkha, A.J., Natural convective boundary layer flow over a nonisothermal vertical plate embedded in a porous medium saturated with a nanofluid, *Nanoscale and Microscale Thermophysical Engineering*, 15(2), 2010, 81-94.
[78] Chamkha, A.J., Abbasbandy, S., Rashad, A.M., Vajravelu, K., Radiation effects on mixed convection about a cone embedded in a porous medium filled with a nanofluid, *Meccanica*, 48, 2013, 275-285.
[79] Xiao, A.W., Lee, H.J., Capone, I., Robertson, A., Wi T., Fawdon, J., Wheeler, S., Lee, H.W., Grobert, N., Pasta, M., Understanding the conversion mechanism and performance of monodisperse FeF_2 nanocrystal cathode, *Nature Materials*, 19, 2020, 644-654.
[80] Lewis, D.J., Zomberg, L.Z., Carter, D.J.D., Macfarlane, R.J., Single crystal winter bottom constructions of nanoparticles superlattices, *Nature Materials*, 2020, doi: 10.1038/s41563-020-0681-0.
[81] Little, A., Lee, C., John, C., Doyle, S., Maniv, E., Nair, N.L., Chen, W., Rees, D., Venderbos, J.W.F., Fernandes, R.M., Analyts, J., Orenstein, J., Three state nematicity in the triangular lattice antiferromagnetic Fe_2NbS_2, *Nature Materials*, 2020, doi: 10.1038/s41563-020-0681-0.
[82] Wang, S., Zhao, S., Shi, Z., Wu, F., Zhao, Z., Jiang, L., Wanatabe, K., Taniguchi, T., Zetti, A., Zhou, C., Wang, F., Nonlinear luttinger liquid plasmons in semiconducting single –walled carbon nanotubes, *Nature Materials*, 2020, doi: 10.103/1038/s41563-020-0652-5.

ORCID ID

Akinbowale T. Akinshilo https://orcid.org/000-0002-6436-3420
Amin Davodi https://orcid.org/000-0003-2015-6064
Adeleke Ilegbusi https://orcid.org/000-0001-8421-1873
Gbeminiyi Sobamowo https://orcid.org/0000-0003-2402-1423

How to cite this article: Akinshilo A.T., Davodi A., Ilegbusi A., Sobamowo G. Thermal Analysis of Radiating Film Flow of Sodium Alginate using MWCNT Nanoparticles, *J. Appl. Comput. Mech.*, 8(1), 2022, 219–231. https://doi.org/10.22055/jacm.2020.33386.2218